

CrossMark  
click for updates

Cite this: DOI: 10.1039/c4cy01099j

# One-pot synthesis of (*R*)-2-acetoxy-1-indanone from 1,2-indanedione combining metal catalyzed hydrogenation and chemoenzymatic dynamic kinetic resolution†

Otto Långvik,<sup>a</sup> Thomas Sandberg,<sup>b</sup> Johan Wärnå,<sup>c</sup> Dmitry Yu. Murzin<sup>c</sup> and Reko Leino<sup>\*a</sup>Received 25th August 2014,  
Accepted 15th September 2014

DOI: 10.1039/c4cy01099j

www.rsc.org/catalysis

Combination of the regioselective hydrogenation of the prochiral diketone 1,2-indanedione with chemoenzymatic dynamic kinetic resolution of the resulting *rac*-2-hydroxy-1-indanone was investigated. A new simple to operate, one-pot reaction sequence provides the valuable building block (*R*)-2-acetoxy-1-indanone in moderate enantiopurity (86–92% ee) and a competitive isolated yield (39%) compared with a traditional isolated batch reaction approach.

## 1 Introduction

The development of cost efficient, sustainable chemical processes for preparation of chiral building blocks is of paramount importance in contemporary synthetic and industrial organic chemistry. In recent years, one-pot reaction sequences involving various types of cascade, tandem and multi-component reactions have emerged as a topical research area, providing several advantages over conventional multi-step synthetic methods.<sup>1–7</sup> Furthermore, in modern catalysis research, heterogeneous catalysts are receiving increasing attention also in asymmetric fine chemical synthesis with several advantages over their homogeneous counterparts, particularly due to their simpler work-up, catalyst separation and recycling. A particular objective of our ongoing work is the development of selective, one-pot asymmetric synthesis protocols combining heterogeneous metal and enzyme based catalysts separable by filtration, ideally allowing robust access to chiral small molecules.<sup>8–10</sup>

Vicinal hydroxy ketones serve as useful starting materials for various classes of industrially relevant compounds.<sup>11–16</sup> As shown recently, the vicinal hydroxy ketone, *rac*-2-hydroxy-1-indanone (*rac*-2), can be efficiently obtained by regioselective hydrogenation of the corresponding vicinal dione, 1,2-indanedione (**1**).<sup>9,10</sup> In the absence of asymmetric induction,

the hydrogenation reaction produces an equimolar mixture of the two 2-hydroxy-1-indanone enantiomers. In earlier work, we have investigated the chemoenzymatic dynamic kinetic resolution (DKR) of *rac*-2 by use of heterogeneous catalysts.<sup>8</sup> The deprotected chiral reaction product, (*R*)-2-hydroxy-1-indanone, then serves as a vicinal hydroxy ketone building block for further utilization, *e.g.*, for production of *cis*-1-amino-2-indanol, a widely utilized intermediate for pharmaceuticals, chiral catalysts, chiral auxiliaries and chiral resolving agents.<sup>17–24</sup>

The main methodologies traditionally utilized for the preparation of chiral compounds are based on classical racemate resolution, asymmetric synthesis, and kinetic resolution. Enzymatic kinetic resolution of racemic starting materials is a useful tool for obtaining enantiomerically pure products, being, however, limited to the maximum theoretical yield of 50%.<sup>25</sup> In order to overcome this drawback, various types of DKR processes have been developed where the slower reacting enantiomer is racemized spontaneously or by a catalytic process.<sup>26–29</sup> In DKR reactions, then, theoretical yields of 100% can be achieved. For example, the chemoenzymatic DKR of *sec*-alcohols typically utilizing enzymes, such as CALB, in combination with homogeneous ruthenium based racemization catalysts have in recent years emerged as a powerful tool for the synthesis of enantiomerically pure esters and, after deprotection, the corresponding chiral parent alcohols.<sup>30–34</sup>

Examples of heterogeneous or immobilized homogeneous catalytic systems for dynamic kinetic resolution (DKR) processes have, likewise, been reported in the literature.<sup>35–38</sup> Nevertheless, one-pot cascade or tandem type operations combining both the hydrogenation and DKR reactions in single vessels are rare, although a few examples for selected ketoximes and carbonyl compounds have been described.<sup>39–45</sup> In general, while one-pot and cascade-type reaction approaches

<sup>a</sup> Laboratory of Organic Chemistry, Åbo Akademi University, FI-20500 Åbo, Finland.  
E-mail: reko.leino@abo.fi

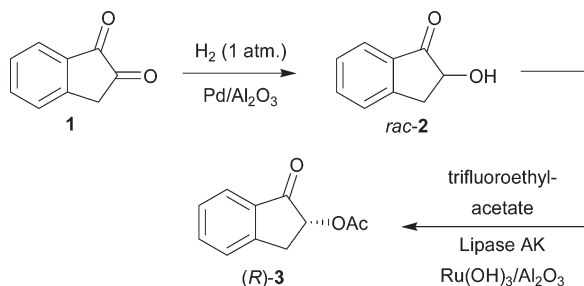
<sup>b</sup> Laboratory of Physical Chemistry, Åbo Akademi University, FI-20500 Åbo, Finland

<sup>c</sup> Laboratory of Industrial Chemistry and Reaction Engineering, Process Chemistry Centre, Åbo Akademi University, FI-20500 Åbo, Finland

† Electronic supplementary information (ESI) available: <sup>1</sup>H-NMR spectra for (*R*)-**3**, **6** and **7**, DFT calculations results, chiral GC chromatograms and Ru catalyst characterization (HR-TEM, TPR, XPS). See DOI: 10.1039/c4cy01099j

ideally result in overall more efficient chemical processes, reducing also the number of work-up stages required, the combination of different types of catalysts, *e.g.*, chemical and enzymatic, into a single reaction vessel often remains challenging. For example, the combination of regioselective hydrogenation with subsequent DKR reaction is particularly demanding, especially in terms of retaining the catalytic activities and selectivities of the different catalysts involved throughout the whole reaction process. Thus, mutually compatible tailored catalyst combinations are required, not undergoing severe catalyst inactivation or poisoning pathways induced by the reaction products, starting materials or intermediates. Ideally, this type of heterogeneous reaction sequences could also further be converted to flow type systems,<sup>46–48</sup> receiving increasing interest both in industry and academic laboratories in recent years.<sup>49–54</sup>

In the present paper, we describe our work on the combination of the two earlier published reactions by us, namely, the regioselective hydrogenation of 1,2-indanedione<sup>9</sup> and the chemoenzymatic dynamic kinetic resolution of *rac*-2 (ref. 8) into a new one-pot reaction sequence (Scheme 1). Initial experiments were also carried out on the potentially regioselective hydrogenation of two other vicinal diketones, 9,10-phenanthrenequinone and 1,2-naphthoquinone. Limitations and scope of the one-pot approach are discussed.



**Scheme 1** One-pot reaction combining the regioselective hydrogenation of 1,2-indanedione (**1**) and chemoenzymatic dynamic kinetic resolution of the intermediate *rac*-2-hydroxy-1-indanone (*rac*-2) producing (*R*)-2-acetoxy-1-indanol [(*R*)-**3**].

## 2 Experimental

### 2.1 Materials

The starting material **1** was prepared according to literature procedures with <sup>1</sup>H and <sup>13</sup>C NMR spectroscopic data and melting point identical to those reported previously.<sup>55–59</sup> The other diketones, 1,2-naphthoquinone (**4**) (97%) and 9,10-phenanthrenequinone (**5**) (95%), were purchased from Sigma-Aldrich and used without further purification. The Pd/Al<sub>2</sub>O<sub>3</sub> catalyst used for the hydrogenation reactions was purchased from Aldrich (product 205710; 5 wt% Pd) and sieved prior to use (<63 μm). The enzyme, lipase AK (from *Pseudomonas fluorescens*), was purchased from Sigma-Aldrich and used after immobilization on celite and in trial reactions without immobilization. The immobilization of lipase AK on celite was carried out as described in the literature using

10% (w/w) lipase and 5% (w/w) sucrose.<sup>60</sup> Ru(OH)<sub>3</sub>/Al<sub>2</sub>O<sub>3</sub> was prepared according to literature procedures.<sup>8,61</sup> The hydrogen and argon gases used were of high quality grade, 99.999% and 99.9999%, respectively (Linde Gas – AGA).

### 2.2 Catalyst characterization

The metal loading of the Ru catalyst was determined by using an inductively coupled plasma optical emission spectrometer (ICP-OES; PerkinElmer, Optima 5300 DV) working at λ = 240.272 nm. The ICP sample (16 mg) was applied in a teflon bomb together with *aqua regia* (2.5 mL) and HF (0.5 mL). The sample was digested in a microwave oven (Anton Paar, Multiwave 3000) and diluted to 100 mL volume with deionized water (18 MΩ) prior to analysis. The Ru catalyst samples for high resolution transmission electron spectroscopy (HRTEM) analyses were prepared as a suspension in ethanol, and for calculating the diameter of particles, more than 100 particles for each sample were taken (in one or more pictures). The HRTEM measurements were performed with LEO 912 Omega, voltage 120 kV. The metal dispersion of the Pd catalyst was determined by applying CO pulse chemisorption method using Micromeritics Auto-Chem 2900 apparatus. The Pd dispersion was calculated assuming an adsorption stoichiometry of 1/1 for CO/Pd.<sup>62</sup> The specific surface area of the Pd/Al<sub>2</sub>O<sub>3</sub> catalyst was measured by nitrogen physisorption using an automatic physisorption apparatus (Sorptomatic 1900, Carlo Erba Instruments). BET method was used for calculation of the surface area. The catalyst was degassed prior to the surface area measurement in vacuum at 150 °C. Temperature programmed reduction (TPR) of the Ru(OH)<sub>3</sub>/Al<sub>2</sub>O<sub>3</sub> catalyst was performed with an AutoChem Micromeritics apparatus by using the following temperature ramp: 10 °C min<sup>-1</sup> to 400 °C. X-Ray photoelectron spectroscopy (XPS) was conducted with Karto Axis Ultra electron spectrometer equipped with a delay line detector. The binding energy scale was referenced to the C 1s first line of aliphatic carbon, set at 285.0 eV. Processing of the spectra was accomplished with the Kratos software.

### 2.3 Quantum mechanical calculations

The TURBOMOLE program package<sup>63,64</sup> version 6.1 was used for conducting the quantum mechanical calculations determining the optimized structure of **1**. The calculations were performed by applying density functional theory<sup>65</sup> with the B3LYP hybrid exchange-correlation functional<sup>66–68</sup> in combination with the MARI-J approximation<sup>69–71</sup> and the TZVP basis set<sup>72</sup> for all atoms, as implemented in the TURBOMOLE program package. For determining the charge delocalization in **1**, the GAMESS software<sup>73</sup> was applied using the Hartree-Fock (HF) theory<sup>74</sup> with the basis set 6-31G\*<sup>75–77</sup> obtaining corresponding electrostatic potential fit (ESP) charges.

### 2.4 Reaction setup

The hydrogenation and one-pot reactions were conducted in a five-necked 100 mL round-bottom flask equipped with a mechanical stirrer (gas tight adaptor), gas inlet (7 μm gas

dispenser merged in the solvent), *in situ* thermocouple recording the temperature, funnel (with degassing capability), rubber septa for sampling and condenser further connected to an oil bubbler for gas outlet. The one-pot reactions were performed using hydrogen gas under atmospheric pressure at 40 °C. The Pd catalyst for hydrogenation was pretreated under H<sub>2</sub> flow (1 atm.) for 2 h at elevated temperature (250 °C) in order to ensure that all active metal is in metallic form (oxidation state zero).<sup>9,43</sup> Efficient stirring (500 rpm) and small hydrogenation catalyst particle size (<63 μm) were employed to obtain data in the kinetic regime without external and internal mass transfer limitations. After Pd-catalyst pretreatment, the reaction vessel was cooled down and the degassed (three vacuum-argon cycles) Ru(OH)<sub>3</sub>/Al<sub>2</sub>O<sub>3</sub>, lipase AK and 4 Å molecular sieves were introduced.

### 2.5 Hydrogenation of 1,2-naphthoquinone and 9,10-phenanthrenequinone

The hydrogenations of 1,2-naphthoquinone (4) and 9,10-phenanthrenequinone (5) were performed by dissolving 1.2 mmol of 4 or 5 in 60 mL ethyl acetate (EA). The hydrogenation reactions were started by introducing the deoxygenated solution into the reaction vessel with H<sub>2</sub>-flow atmosphere (1 atm.) containing the Pd/Al<sub>2</sub>O<sub>3</sub> catalyst (51.1 mg, 2 mol% Pd). After 2.5 h reaction time at 40 °C, an *in situ* derivatization was applied by addition of 1 mL acetic anhydride and 1 mL pyridine whereafter stirring was continued for 20 min. The products were separated after filtration of the catalyst, by traditional column chromatography using EA:hexane mixture as the eluent. The isolated yields for 1,2-diacetoxynaphthalene (6) was 85% and for 9,10-diacetoxypheanthrene (7) 78%.

### 2.6 One-pot reaction sequence

In the one-pot reaction sequence 1,2-indanedione (175 mg, 1.2 mmol) and dodecane as an internal standard (68 μL, 0.3 mmol) were dissolved in ethyl acetate (EA), 60 mL, and transferred to a funnel directly connected to the hydrogenation vessel. Deoxygenation of the solution was carried out in the funnel by bubbling with H<sub>2</sub> (15 min) shortly before reaction. The reaction was started by introducing the deoxygenated solution into the reaction vessel with H<sub>2</sub> atmosphere containing the Pd catalyst (51.2 mg, 2 mol%), lipase (125 mg), Ru-catalyst (85 mg, 1.5 mol%) and pre-dried molecular sieves (30 mg), ensuring dry reaction conditions. Trifluoroethyl acetate (545 μL, 4.8 mmol, 4 equivalents) was introduced to the reaction mixture in the reactor 15 min after the reaction had started in five portions with 30 min intervals through the septa using a syringe. It should be noted, however, that *for the kinetic experiments*, in order to simplify the experimental procedure, the full amount of the acyl donor was added directly in the beginning of the reactions. This data, then, was used for plotting of the concentration profiles (Fig. 1–4) and calculation of the kinetic parameters (Table 3). The hydrogen flow rate during the reactions was 25–35 mL min<sup>-1</sup> and the reaction mixtures were kept at 40 °C using a PEG-bath. Prior to product isolation,

the catalysts were removed by filtration through Celite. Chromatographic separation was performed using automated flash system (CombiFlash Companion) equipped with a 4 g (20–40 μm) silica column using EA:hexane as the eluent system (gradient program). Yield of the product (*R*)-2-acetoxy-1-indanol according to GC chromatogram was 51% (peak area) and the isolated yield was 39% (89 mg, 0.47 mmol), colorless oil.

### 2.7 Product analyses

Samples (0.15 mL) from the reactor were taken through a gas tight septum, filtered using a 0.2 μm syringe filter and diluted with three parts of the same solvent after which 1 μL of the solution was injected to the gas chromatograph. The product distribution was monitored by GC or GC/MS. The GC apparatus used was Agilent Technologies 6850 GC equipped with a Varian CP-7502 column (25.0 m × 250 μm × 0.25 μm), 1/50 split, FID detector and He was applied as a carrier gas. The chiral-GC analyses were conducted using the following temperature program: injector 230 °C, detector 280 °C, oven  $T_{\text{initial}} = 130$  °C (0 min), rate 2.2° min<sup>-1</sup>,  $T_{\text{final}} = 185$  °C (10 min). The GC/MS apparatus used was Agilent Technologies 7890 A GC equipped with 5975 C MS detector (EI), HP-5MS column (30 m × 250 μm × 0.25 μm), 1/50 split and He as a carrier gas. The NMR spectra of the isolated compounds were recorded on a Bruker Avance 600 MHz NMR spectrometer equipped with a BBI-5 mm-Zgrad-ATM probe at 25 °C operating at 600.13 MHz for <sup>1</sup>H and 150.92 MHz for <sup>13</sup>C.

## 3 Results and discussion

### 3.1 Catalyst characterization

Based on the ICP-OES results, the heterogeneous Ru(OH)<sub>3</sub>/Al<sub>2</sub>O<sub>3</sub> catalyst contains a 1.9% (w/w) metal loading. The mean Ru-particle size, based on high resolution TEM, was determined to 1.3 ± 0.4 nm. The TPR of the catalyst confirms that no reduction takes place at temperatures below 70 °C in H<sub>2</sub> atmosphere and that the maxima for the H<sub>2</sub> uptake is at 137, 244, and 338 °C.<sup>8</sup> The XPS data displayed binding energy peaks at 463.5 and 485.7 eV defining the oxidation state of the ruthenium species to +III, *i.e.*, Ru(OH)<sub>3</sub>/Al<sub>2</sub>O<sub>3</sub>.<sup>8</sup>

The values for the metal dispersion and the corresponding average metal particle sizes of the Pd-catalyst were determined to be 22% and 5.1 nm, respectively. The BET specific surface area of the Pd catalyst is, according to nitrogen physisorption measurements, 174 m<sup>2</sup> g<sup>-1</sup>.

### 3.2 Hydrogenation

The utilization of 1 as a starting material for further synthetic applications is attractive. This compound is readily available, in part due to its application as a forensic fingerprint reagent.<sup>78,79</sup> Our recently reported regioselective hydrogenation of 1 is an efficient and practical method for preparation of *rac*-2 (Scheme 2)<sup>9</sup> compared with the traditional literature route starting from 1-indanone, providing *rac*-2 after hydrolysis of the corresponding 2-diazo-1-indanone, in turn obtained by oxidation of the 2-oximino-1-indanone intermediate.<sup>55,58</sup>

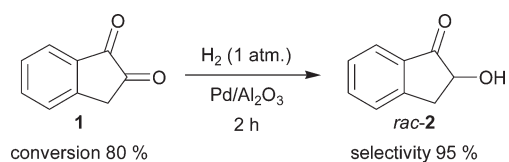
In our earlier study, the regioselective hydrogenation was investigated and the influence of some fundamental reaction parameters, including the choice of the solvent and catalyst, were determined.<sup>9</sup> Conclusively, by using EA as the solvent and Pd/Al<sub>2</sub>O<sub>3</sub> (2 mol%) as the catalyst, reproducible results were obtained with **1** being reduced to *rac*-**2** with very high initial selectivity (99%) at up to 50% conversion. At longer reaction times, higher conversions were achieved at lower selectivity due to consecutive hydrogenation. Nevertheless, acceptable selectivities (92%) towards the desired alcohol were obtained at a reasonably high (84%) conversion level (Table 1, entries 1–4).<sup>9</sup>

### 3.2.1 Antiaromatic character of 1,2-indanedione.

Preliminary quantum mechanical calculations were carried out in order to elucidate the potentially antiaromatic character of the starting material **1**. According to literature, antiaromatic compounds contain  $4n$  ( $n \neq 0$ )  $\pi$ -electrons in a cyclic and planar or nearly planar system consisting of alternating single and double bonds.<sup>80</sup> Three additional characteristics possessed by antiaromatic compounds are: 1) decreased thermodynamic stability; 2) tendency to alternation of bond lengths; and 3) small energy gap between the highest occupied (HOMO) and the lowest unoccupied molecular orbitals (LUMO).<sup>80</sup> Tyutyulkov and coworkers have earlier performed quantum chemical calculations for the enolic anion form of **1**, with results supporting the antiaromatic character of the anionic structure.<sup>81</sup> In the earlier study, some characteristic properties of antiaromatic structures, including Jahn–Teller distortion, negative net charge in the five-membered carbon ring and spectroscopic data supporting the proposal of a small band gap between the HOMO–LUMO, were observed.<sup>81</sup> Furthermore, compound **1** and the related reactive radical structures have been studied using electron spin resonance by other investigators.<sup>82–84</sup>

As the tendency to alternation of bond lengths is one of the characteristics possessed by antiaromatic compounds, the bond lengths of **1** were evaluated here using quantum mechanical calculations with the TURBOMOLE program package (for details, see experimental section). The calculations performed clearly indicate the unmodified structure **1** to be less antiaromatic compared to its enolic counterpart with the calculated bond lengths of **1** not significantly differing from the expected ones, also not indicating any significant Jahn–Teller distortions (Fig. S3, ESI†).

As the benzylic charge delocalization likely results in different atomic charges on the carbonyl groups in position 1 and 2, and is likely to influence the chemical behaviour of



**Scheme 2** Hydrogenation of **1** to *rac*-**2** with H<sub>2</sub> using Pd/Al<sub>2</sub>O<sub>3</sub> (2 mol%) as the catalyst.

**Table 1** Conversion and selectivity for the hydrogenation of **1** (1.2 mmol) to *rac*-**2** using Pd/Al<sub>2</sub>O<sub>3</sub> catalyst (51.1 mg, 2 mol%)

Entry	Conversion of <b>1</b> [%]	Selectivity towards <i>rac</i> - <b>2</b> [%]
1	56	99
2	84	92
3	87	87
4	90	42

compound **1** in the hydrogenation reaction, the atomic charges were calculated (for details, see Experimental section). While the difference between the atomic charges of the two carbonyl carbons is moderate, the results obtained support the earlier suggested property of delocalization of the benzylic C=O double bond to the aromatic region and thus resulting in the relatively higher reactivity of the carbonyl group in position 2 (Fig. S4, ESI†). However, in order to fully explain the behaviour of **1** in the heterogeneously catalyzed hydrogenation reactions, more thorough calculations would be needed, including calculations of the different adsorption modes of the substrate to the catalyst surface.

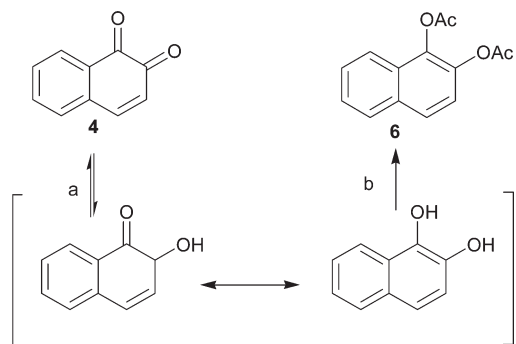
Conclusively, as indicated by the results obtained herein, the non-ionized form of **1** shows only one antiaromatic feature, namely the small band gap between the HOMO and LUMO,  $-0.246 E_h$  and  $-0.110 E_h$ , respectively.

### 3.3 One-pot hydrogenation and esterification of 1,2-naphthoquinone and 9,10-phenanthrenequinone

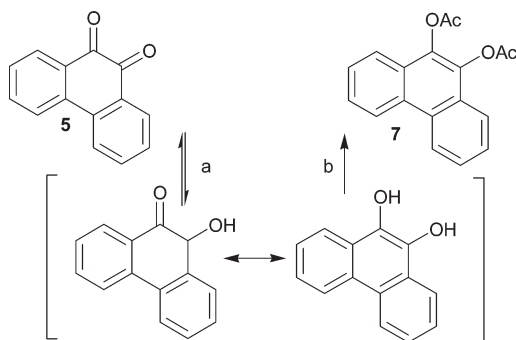
In order to further develop and apply the regioselective hydrogenation of vicinal diketones to other potential structures, preliminary hydrogenation studies were carried out by using **4** and **5** as the starting materials. These hydrogenations were initially carried out under similar reaction and pretreatment conditions as used for **1**. While investigating the hydrogenation of **5**, it became evident, however, that the conditions used for **1** were not applicable for this compound. In the GC analysis, no product was observed although during the hydrogenation reaction a clear color change from yellow to colorless, characteristic for diones, was observed. The disappearance of the product was then shown to result from back-oxidation of the product to starting material in air atmosphere prior to analysis. The reduction-oxidation equilibrium shifts rapidly towards the oxidized form upon exposure to air after venting of the hydrogenation reactor. An *in situ* derivatization, by acylation, was applied in order to avoid oxidation of the products and also enabling easier separation and increasing the isolated yield. This sequence provided, for the two different starting materials, the corresponding diacetates **6** and **7** in isolated yields of 85% and 78%, respectively (Schemes 3 and 4). The isolated diacetate products are likely formed by rearrangement of the hydroxy ketones by proton transfer and subsequent aromatization (Schemes 3 and 4).

The hydrogenation and derivatization or protection of the diols formed, *i.e.*, reductive acetylation, is a well-known transformation for quinone type structures.<sup>85–88</sup> Hydrogenations of compounds **4** and **5** initially proceed similar to that of **1**, possibly forming hydroxy ketones as intermediates, which then

are rapidly and spontaneously rearranged to form more stable and energetically favored aromatic diols, or alternatively are easily oxidized back to the starting material. Notably, because of the symmetric structure of **5** the hydrogenation cannot proceed in a regioselective manner. Nevertheless, the successful *in situ* derivatizations of the reaction products indicate that the envisioned conceptually related one-pot hydrogenation and esterification sequence should be feasible.



**Scheme 3** Hydrogenation (a) and subsequent esterification (b) of **4** to **6** with H<sub>2</sub> (1 atm.) and Pd/Al<sub>2</sub>O<sub>3</sub> as catalyst.



**Scheme 4** Hydrogenation (a) and subsequent esterification (b) of **5** to **7** with H<sub>2</sub> (1 atm.) and Pd/Al<sub>2</sub>O<sub>3</sub> as catalyst.

### 3.4 Dynamic kinetic resolution

Lipase catalyzed kinetic resolution is a powerful tool for production of enantiomerically pure compounds. Prerequisites for a viable resolution process include the correct selection of a suitable enzyme, active acyl donor, low water content in the reaction media and rapid *in situ* racemization of the starting material. The most efficient *sec*-alcohol racemization catalysts developed to date are based on soluble half-sandwich ruthenium complexes.<sup>89–91</sup> For these homogeneous catalysts, strictly anhydrous and oxygen-free reaction conditions are often required. Moreover, efficient procedures for separation and recycling of the homogeneous catalysts are seldom available.

Heterogeneous catalysts, in general, enable easier recycling by simple filtration. Several examples of heterogeneous DKR processes have been reported in literature.<sup>35,92–96</sup> The majority of the heterogeneously catalyzed DKRs utilize transition metal, Brønsted or Lewis acid based racemization catalysts.<sup>35,92–96</sup> Furthermore, some of these heterogeneously

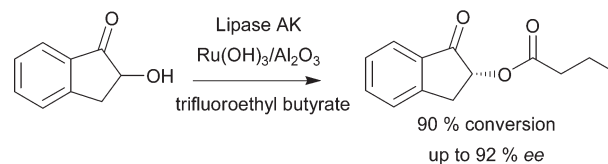
catalyzed DKR reactions have been converted into flow type reaction applications.<sup>46–48</sup> In the literature, the reported one-pot catalyst systems suffer, however, from often reduced catalytic activities. The racemization catalysts may be inhibited to various degrees by the starting materials or products.<sup>8,45</sup> Activity of the enzyme may, in turn, be inhibited by acidic catalysts used for racemization.<sup>92,93</sup>

During our development of the chemoenzymatic DKR of *rac*-**2**,<sup>8</sup> several potential racemization catalysts were investigated. In addition to the catalysts studied in the earlier paper, we have now additionally investigated VOSO<sub>4</sub> for racemization of (*S*)-**2**. Racemizations of various benzylic alcohols using VOSO<sub>4</sub> have been reported earlier.<sup>94</sup> Racemization of (*S*)-**2** (0.02 M) at 40 °C using EA as the solvent in the presence of 0.02 M VOSO<sub>4</sub> proved, however, unsuccessful and any significant racemization could not be detected during the course of a 5 h reaction. The previously developed heterogeneously catalyzed DKR,<sup>8</sup> converting *rac*-**2** into (*R*)-1-oxoindan-2-yl-butanoate (Scheme 5) in 85–90% conversion and up to 92% *ee* was, therefore, considered sufficiently efficient for combining the DKR with hydrogenation experiments.

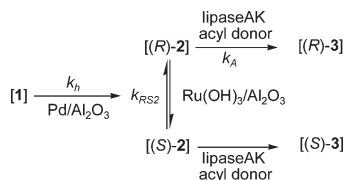
### 3.5 One-pot combination of hydrogenation and DKR

The primary aim of the present work was to combine the earlier described regioselective hydrogenation of **1** and the DKR of *rac*-**2** into a one-pot reaction sequence (Scheme 6). The results are presented in Table 2. An interesting observation during the earlier reported DKR (Scheme 5) was the minor formation of **1** as an undesired by-product.<sup>8</sup> The aim here was to employ reductive reaction conditions and to utilize catalytic hydrogenation of compound **1**, a more benign and accessible starting material compared to *rac*-**2**, further to *rac*-**2** producing after DKR the desired chiral product (*R*)-**3**.

The initial one-pot experiments combining the hydrogenation and DKR were conducted by switching the reaction atmosphere from hydrogen gas to argon during the reaction, similar to the earlier reported, conceptually related one-pot type reaction sequence of Bäckvall and co-workers.<sup>41</sup> Thus, in the first experiments performed here, the gas feed was changed from hydrogen to argon after two hours of reaction. In this time, the earlier reported regioselective hydrogenation proceeds rapidly providing reasonable conversion.<sup>9</sup> In this work it became evident, however, that the introduction of argon did not enhance the conversion or selectivity of the one-pot reaction sequence. Therefore, in further experiments only hydrogen gas was used. For selection of solvent, methyl-*tert*-butyl ether (MTBE) and EA were considered. While MTBE



**Scheme 5** DKR of *rac*-**2** using Ru(OH)<sub>3</sub>/Al<sub>2</sub>O<sub>3</sub> as the racemization catalyst in combination with lipase AK yielding (*R*)-1-oxoindan-2-yl-butanoate with high *ee* 92% and 90% conversion.<sup>8</sup>



**Scheme 6** One-pot reaction sequence including: i) hydrogenation of **1**; ii) racemization of (*S*)-**2** and (*R*)-**2**; iii) acylation of the formed (*R*)-**2** with acyl donor forming (*R*)-**3**.

was initially used with good results for the DKR, as reported earlier,<sup>8</sup> EA was here found more suitable for the one-pot sequence with better dissolution properties for starting material **1** compared to MTBE. The ether required surprisingly long time to dissolve **1** at the desired concentrations and at higher concentrations resulted in slightly hazy solutions, also observed earlier in the hydrogenation reaction.<sup>9</sup>

In the one-pot sequence reactions using EA as the solvent and trifluoroethyl butyrate (**8**) as the acyl donor, we observed, not surprisingly, both the corresponding acetate and butanoate products in 1.7 : 1, product ratios, respectively. In previous work, Park and co-workers have reported the utilization of EA in a dual role, both as an acetyl donor and a solvent, in lipase catalyzed esterification reactions.<sup>97–99</sup> Generally, a significant molar excess of the solvent acting as the acetyl donor compared to the amount of substrate drives the reaction equilibrium heavily to the right without a substantial backward reaction. In the one-pot sequence reactions investigated here, the use of EA as the acetyl donor also proved feasible at first, retaining the high product *ee* (>90% after 21 h) value throughout the whole reaction (Table 2, entry 2) in the absence of other acyl donors. For increasing the conversion and yield, an activated acetyl donor was desirable. Therefore, trifluoroethyl acetate (**9**) was added to the one-pot sequence reaction mixture. By carrying out one-pot reactions with further increased amounts of acyl donor, the yield consequently increased as expected (Table 2, entries 3–5).

To further study the advantages and limitations of the one-pot reaction sequence, reactions with different enzyme amounts (93, 130, and 163 mg) were performed. Changes in the enzyme amount were expected to influence the reaction rate of the lipase AK catalyzed resolution of the *rac*-**2** intermediate to the acetylated end product ( $k_A$ , Scheme 6). In order to produce an efficient DKR type reaction, the *ee* value should be kept as low as possible for compound **2**. Therefore, the change in the acetylation rate was consequently assumed to influence the (*R*)-**2** : (*S*)-**2** ratio ( $k_A : k_{RS2}$ ). The rate by which the acetylated end product was formed ( $k_A$ ) was, nevertheless, influenced only slightly by the variation of the enzyme amount (Fig. 1). Subsequently, the concentrations of the components in the three separate one-pot reactions are similar. One example of the kinetic curves obtained is shown in Fig. 2 (130 mg lipase AK). Conclusively, these results demonstrate that the enzyme catalyzed resolution in the one-pot sequence is not the rate limiting step and good kinetic resolution is accomplished with the reaction conditions applied.

**Table 2** One-pot sequence combining hydrogenation and DKR producing (*R*)-**3** from **1** (1.2 mmol) over Pd/Al<sub>2</sub>O<sub>3</sub> (2.0 mol%)

Entry	Solvent	Acyl donor <sup>a</sup> (equivalents)	Yield <sup>b</sup> [%]	<i>ee</i> <sup>b,c</sup> [%]
1	MTBE	8 (3,7)	52	28
2	EA	—	34	90
3	EA	9 (1)	33	91
4	EA	9 (2.5)	40	86
5	EA	9 (4) <sup>d</sup>	51	86

<sup>a</sup> Number of equivalents acyl donor related to the amount starting material **1**. <sup>b</sup> According to GC chromatogram. <sup>c</sup>  $ee = 100 \cdot \frac{[(R)-3] - [(S)-3]}{[(R)-3] + [(S)-3]}$ . <sup>d</sup> Added in portions.

The limiting step in the one-pot reaction appears to be, at least partially, the hydrogenation of compound **1** to *rac*-**2**. This was somewhat unexpected, as in the earlier work on regioselective hydrogenation,<sup>9</sup> a long reaction time (20 h) resulted in high (>85%) conversion of **1**. The high conversion (>85%) in turn resulted in significantly decreased selectivity (less than 40%) due to the consecutive hydrogenation of *rac*-**2**

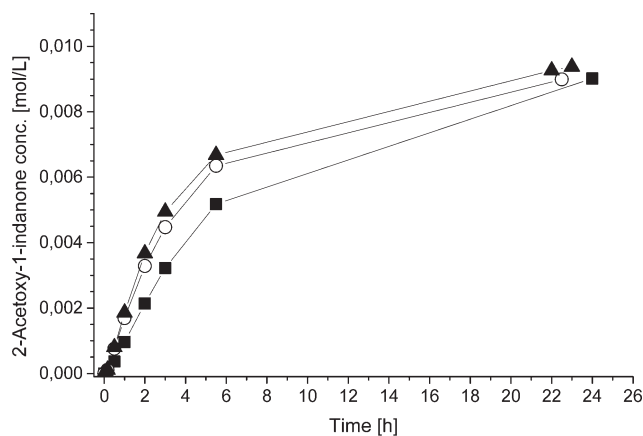


**Fig. 1** 2-Acetoxy-1-indanone concentration during the one-pot reactions using ■ 93 mg, ○ 130 mg and ▲ 163 mg of lipase AK, 51.6–51.9 mg Pd/Al<sub>2</sub>O<sub>3</sub>, 89.5–90.1 mg Ru(OH)<sub>3</sub>/Al<sub>2</sub>O<sub>3</sub> and 4 equivalents (550 μL) of the acyl donor **9** at 40 °C.

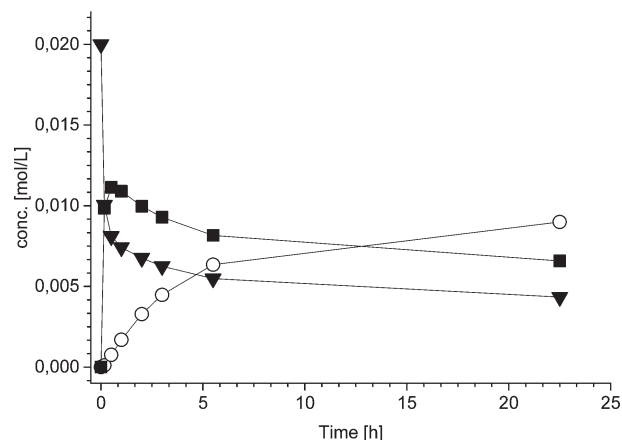


**Fig. 2** Concentration profiles of ▼ 1,2-indanedione, ■ 2-hydroxy-1-indanone, ○ 2-acetoxy-1-indanone for one-pot reaction using 51.6 mg Pd/Al<sub>2</sub>O<sub>3</sub>, 89.5 mg Ru(OH)<sub>3</sub>/Al<sub>2</sub>O<sub>3</sub>, 130 mg lipase AK and 4 equivalents (550 μL) of the acyl donor **9** at 40 °C.

to diols.<sup>9</sup> During the development of the one-pot reaction sequence described here, the 2 mol% loading of Pd was considered to be sufficiently high for obtaining satisfactory reaction rates while avoiding the diol formation from over hydrogenation. Suppression of the consecutive hydrogenation to diols is particularly essential in the one-pot approach where, in the presence of an enzyme, lipase catalyzed acetylation of the isomeric alcohols would result in undesired mixtures of acetylated products.

Additionally, also the racemization rate ( $r_{RS2}$ ) decreases under the applied one-pot conditions resulting in increased *ee* of the 2-hydroxy-1-indanone intermediate (Fig. 3). The compounds present in the one-pot reaction sequence, particularly the esterified product, appear to inhibit the  $\text{Ru}(\text{OH})_3/\text{Al}_2\text{O}_3$  racemization catalyst as shown in Fig. 3(A), where *ee* of the intermediate compound 2 vs. the concentration of the 2-acetoxy-1-indanone end product exhibit linear dependence. However, the amount of the enzyme catalyst is not influencing the racemization rate. Similar observations have been made in earlier studies, suggested to be a consequence of the adsorption of the esters present in the reaction mixture on the heterogeneous Ru catalyst surface active sites.<sup>8,43</sup>

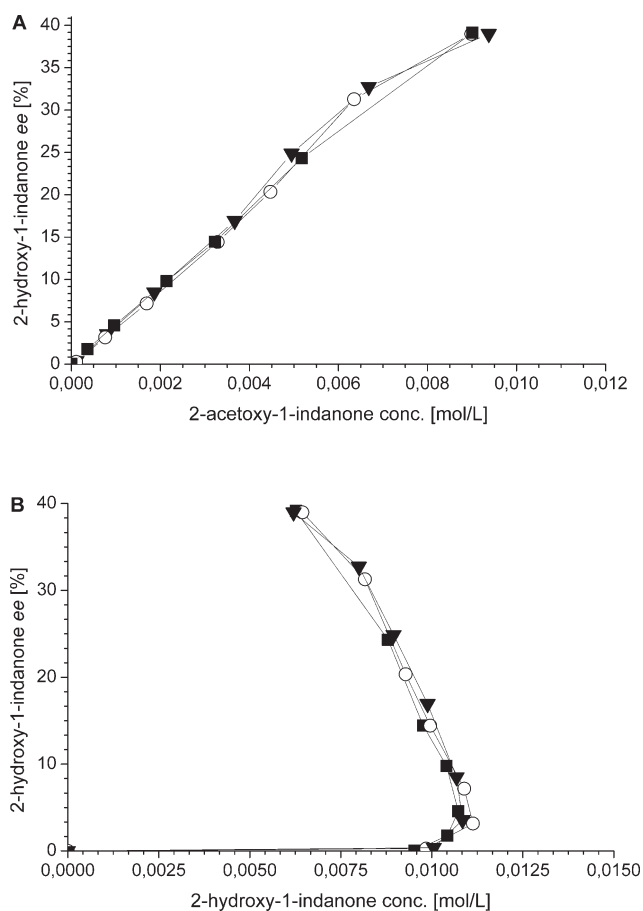


**Fig. 3** (A) Enantiomeric excess ( $ee = 100 \cdot ((R)-3) - ((S)-3) / ((R)-3) + ((S)-3)$ ) of 2-hydroxy-1-indanone versus concentration of 2-acetoxy-1-indanone in one-pot reactions using ■ 93 mg, ○ 130 mg and ▼ 163 mg lipase AK; (B) enantiomeric excess (*ee*) of 2-hydroxy-1-indanone versus 2-hydroxy-1-indanone concentration in one-pot reactions using ■ 93 mg, ○ 130 mg and ▼ 163 mg lipase AK.

Hence, in order to improve the conversion and yield and to decrease the influence of the acyl donor (9) on the racemization catalyst activity, the acetyl donor was added in five portions during the first two hours of the reaction, providing the end product in 51% yield (according to GC). The stepwise addition of the acyl donor also further enhanced the efficiency of the racemization catalyst  $\text{Ru}(\text{OH})_3/\text{Al}_2\text{O}_3$  to some degree. Despite of this, the intermediate product 2 in the one-pot sequence did not remain fully racemic throughout the reaction.

Thus, when the one-pot reaction sequence was carried out according to the method described in the Experimental section (see: 2.6 One-pot reaction sequence), acceptable yields and high *ee* values of the product (Table 1) (*R*)-3 were obtained. Overall, at least conceptually, combination of the regioselective hydrogenation of 1 yielding *rac*-2 with the subsequent DKR producing (*R*)-3 enables an efficient reaction operation without the need for separation of the intermediate hydrogenation product. Furthermore, the reductive reaction conditions employed here enhance the efficiency of the DKR of *rac*-2, eliminating the formation of the oxidized DKR byproduct reported previously.<sup>8</sup>

For better understanding of the reaction network, kinetic modelling of the one-pot process was performed with three different concentrations of the enzyme.

The following rate equations were used:

$$r^{(h)} = \frac{k_h K_1 C_1}{1 + K_1 C_1 + K_{AD} C_{AD}} \rho_{Pd} \quad (1)$$

$$r^{(R2 \rightarrow R3)} = \frac{k_{R3} K_{R2} K_{AD}^E C_{R2} C_{AD}}{1 + K_{R2} C_{R2} + K_{S2} C_{S2} + K_{AD}^E C_{AD}} \rho_{En} \quad (2)$$

$$r^{(S2 \rightarrow S3)} = \frac{k_{S3} K_{S2} K_{AD}^E C_{S2} C_{AD}}{1 + K_{R2} C_{R2} + K_{S2} C_{S2} + K_{AD}^E C_{AD}} \rho_{En} \quad (3)$$

$$r^{(S2 \rightarrow R2)} = \frac{k_{RSA} K_{S2} C_{S2}}{1 + K_{AD}^{Ru} C_{AD}} \rho_{Ru} \quad (4)$$

$$r^{(R2 \rightarrow S2)} = \frac{k_{RSA} K_{R2} C_{R2}}{1 + K_{AD}^{Ru} C_{AD}} \rho_{Ru} \quad (5)$$

In eqn (1)  $k_h$  is a lumped constant containing also the hydrogen concentration,  $C_1$  and  $K_1$  denote concentrations of compound 1 and its adsorption coefficient on Pt. Besides the reactant, also the acylation agent was assumed to be adsorbed on the platinum surface with the adsorption coefficient  $K_{AD}$ . This was included in the model due to the nature of the acyl donor, which can block the catalyst surface, thereby decreasing the catalyst activity. The enzymatic reactions  $r^{(R2 \rightarrow R3)}$  and  $r^{(S2 \rightarrow S3)}$  were assumed to proceed by binding of both reagents in a mechanism conceptually similar to sequential bisubstrate reactions. Finally, for the racemization reactions, adsorptions of (*R*)-2 and (*S*)-2 were considered to be inferior to the much stronger adsorption of the acyl

donor. In eqn (1)–(5)  $\rho_{Ru}$ ,  $\rho_{Pd}$ ,  $\rho_{En}$  etc., correspond to the bulk densities of ruthenium, palladium and lipase, respectively.

The generation rates for the compounds can be subsequently written

$$\begin{aligned} -\frac{dC_1}{dt} &= r^{(h)}, \quad \frac{dC_{R3}}{dt} = r^{(R2 \rightarrow R3)}, \quad \frac{dC_{S3}}{dt} = r^{(S2 \rightarrow S3)}, \\ \frac{dC_{R2}}{dt} &= 0.5r^{(h)} - r^{(R2 \rightarrow R3)} - r^{(R2 \rightarrow S2)} + r^{(S2 \rightarrow R2)} \\ \frac{dC_{S2}}{dt} &= 0.5r^{(h)} - r^{(S2 \rightarrow S3)} + r^{(R2 \rightarrow S2)} - r^{(S2 \rightarrow R2)} \end{aligned} \quad (6)$$

The kinetic modelling was performed for all reaction rates and three reaction sets together. For the parameter estimation, a set of differential equations describing the changes in the concentration profiles of the reagents and products with time was solved by means of ModEst software.<sup>100</sup> Using Levenberg–Marquardt simplex method, the target function, which was defined as incompliance between the experimental and calculated values of concentrations was used to solve the system. The sum of the residual squares between the model and the experimental data was minimized using the following objective function;

$$Q = \|x_{\text{exp}} - x_{\text{est}}\|^2 = \sum_i \sum_t (x_{\text{exp},it} - x_{\text{est},it})^2 \quad (7)$$

where  $x_{\text{exp}}$  is the experimental value and  $x_{\text{est}}$  denotes the predictions given by the model,  $i$  is the component index and  $t$  is the time value. The quality of the fit and accuracy of the model description was defined by the degree of explanation  $R^2$ ; which reflects comparison between the residuals given by the model to the residuals of the simplest model one may think of, i.e., the average value of all the data points. The  $R^2$  value is given by the expression

$$R^2 = 100 \frac{(y_{\text{model}} - y_{\text{experiment}})^2}{(y_{\text{model}} - \bar{y}_{\text{experiment}})^2} \quad (8)$$

Preliminary calculations demonstrated that the description of the hydrogenation reaction is mediocre due to strong catalyst deactivation, which could not be sufficiently well described assuming only adsorption of the acyl donor on Pd surface acting as a catalyst poison.

In previous work,<sup>42</sup> where also hydrogenation and chemoenzymatic DKR were combined in a one-pot fashion, the hydrogenation of acetophenone on palladium was found to undergo strong deactivation, similar to the current case where palladium is inhibited in the hydrogenation of compound 1. For the sake of modelling, an empirical time dependent function for the catalyst activity was proposed.<sup>42</sup> Since a physical meaning in such dependence is unclear it was decided to use a more mechanistically based assumption.

The expression for hydrogenation was modified

$$r^{(h)} = \frac{k_h K_1 C_1}{1 + K_1 C_1 + K_{AD} C_{AD}} \rho_{Pd} q_{\text{deact}} \quad (9)$$

to include the deactivation function<sup>101</sup>

$$q_{\text{deact}} = \frac{C_1 - C_{1,\infty}}{C_1^0 - C_{1,\infty}} \quad (10)$$

where  $C_1$  is the concentration of 1,  $C_1^0$  is the initial concentration of the substrate 1,  $C_{1,\infty}$  is the concentration at infinite time, which was also considered as an adjustable parameter in the data fitting.

The deactivation function, used in earlier work<sup>101</sup> to explain the activity profile in the hydrogenation of cyclohexene, is based on the assumption that a decline in catalyst activity is proportional to the amount of product formed and could be related to catalyst fouling.

Calculations made with eqn (2)–(5) and (9) allowed further simplifications but neglecting adsorption terms in denominators of all rate expressions. The final expressions for the reaction rates are

$$r^{(h)} = k_h K_1 C_1 \rho_{Pd} \frac{C_1 - C_{1,\infty}}{C_1^0 - C_{1,\infty}} = k'_h \rho_{Pd} \frac{C_1 - C_{1,\infty}}{C_1^0 - C_{1,\infty}} \quad (11)$$

$$r^{(R2 \rightarrow R3)} = k_{R3} K_{R2} K_{AD}^E C_{R2} C_{AD} \rho_{En} = k'_{R3} C_{R2} C_{AD} \rho_{En} \quad (12)$$

$$r^{(S2 \rightarrow S3)} = -k_{S3} K_{S2} K_{AD}^E C_{S2} C_{AD} \rho_{En} = k'_{S3} C_{S2} C_{AD} \rho_{En} \quad (13)$$

$$r^{(S2 \rightarrow R2)} = k_{RSA} K_{S2} C_{S2} \rho_{Ru} = k'_{RSA} C_{S2} \rho_{Ru} \quad (14)$$

$$r^{(R2 \rightarrow S2)} = k_{RSA} K_{R2} C_{R2} \rho_{Ru} = k'_{RSA} C_{R2} \rho_{Ru} \quad (15)$$

The estimated values of the parameters as well as the relative standard errors (in %) are presented in Table 3. The fit of the kinetic model to the experimental data for the three different reactions is displayed Fig. 4.

## 4 Conclusions

Combination of the regioselective heterogeneously catalysed hydrogenation of the prochiral diketone 1,2-indandione with dynamic kinetic resolution of the resulting *rac*-2-hydroxy-1-indanone using a heterogeneous Ru catalyst for racemization and an enzyme, lipase AK, for acylation, has been investigated. A new, simple to operate one-pot reaction sequence provides the valuable building block (*R*)-2-acetoxy-1-indanone in moderate enantiopurity (86–92%) in a reasonable reaction time (20 h). In contrast to a multi-step reaction approach in separate reactors, the one-pot, heterogeneously

**Table 3** Estimated parameter values and the corresponding relative standard error. Degree of explanation 92.94%

Parameter	Value	Relative standard error [%]
$k'_h$ [h <sup>-1</sup> ]	3.22	8.1
$k'_{R3}$ [h <sup>-1</sup> ]	$2.09 \times 10^{-3}$	7.0
$k'_{RSA}$ [h <sup>-1</sup> ]	$2.56 \times 10^{-2}$	17.2
$k_{S3}$ [h <sup>-1</sup> ]	$3.52 \times 10^{-5}$	50.9
$C_{1,\infty}$ [mol L <sup>-1</sup> ]	$6.37 \times 10^{-3}$	2.5

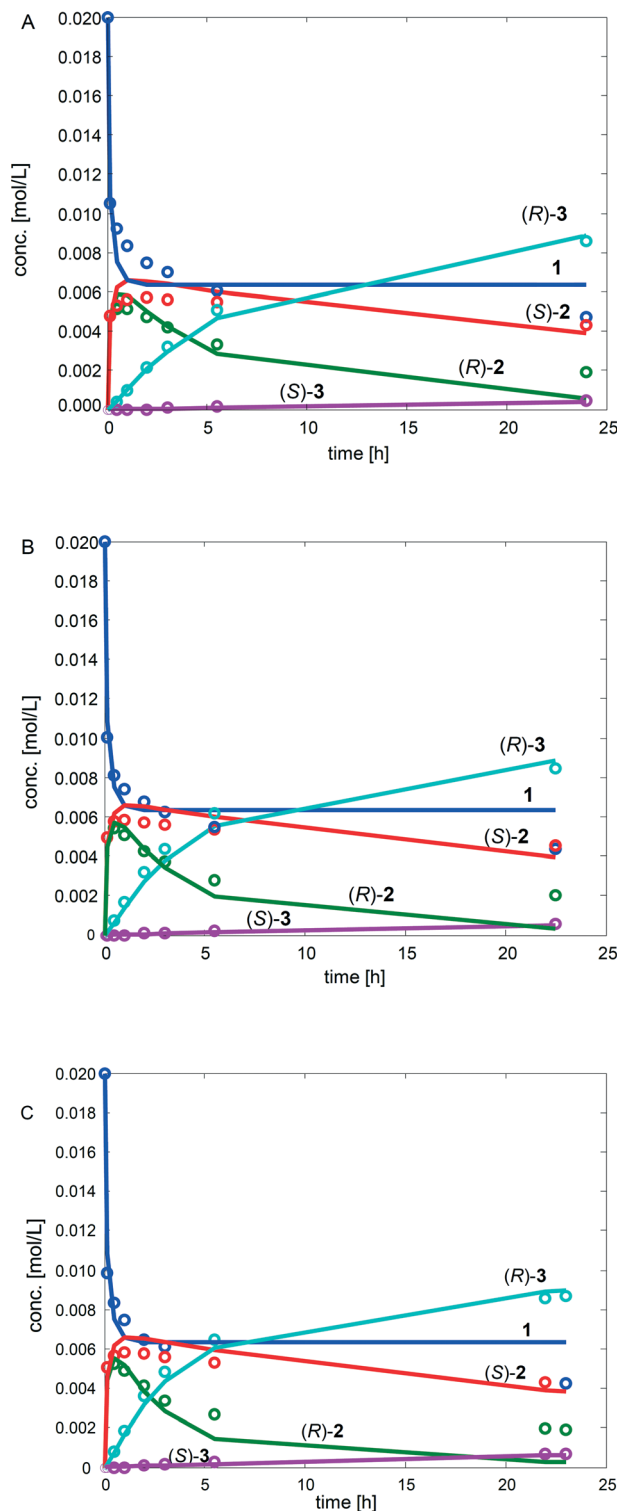


**Fig. 4** Comparison between the experimental data and the model predictions for the reactants in the three one-pot reactions using (A) 93 mg, (B) 130 mg and (C) 163 mg lipase AK. Solid lines represent the estimated data and circles the experimental data. The different compounds are represented by the following colors: blue compound 1, red (S)-2, green (R)-2, cyan (R)-3, pink (S)-3. The degree of explanation 92.94% and the standard errors of the parameters are acceptably low.

catalysed reaction sequence ideally enables simple recovery of the catalysts by filtration facilitating product isolation.

Overall, the readily available 1,2-indanedione can be transferred to a useful chiral building block with high regioselectivity and moderate stereoselectivity using economically viable heterogeneous catalysts in a practical catalytic operation.

## Acknowledgements

The authors thank Alexey Kirilin (Laboratory of Industrial Chemistry and Reaction Engineering, Åbo Akademi University) for preparation of the  $\text{Ru}(\text{OH})_3/\text{Al}_2\text{O}_3$  catalyst and temperature programmed reduction analyses. The authors also thank Sten Lindholm (Laboratory of Analytical Chemistry, Åbo Akademi University) for ICP analyses, Päivi Mäki-Arvela (Laboratory of Industrial Chemistry and Reaction Engineering, Åbo Akademi University) for the CO pulse chemisorption analyses, Atte Aho (Laboratory of Industrial Chemistry and Reaction Engineering, Åbo Akademi University) for nitrogen physisorption analyses and Krisztian Kordas and Anne-Riikka Leino (Microelectronics and Materials Physics Laboratories, Department of Electrical and Information Engineering, University of Oulu) for the HRTEM analyses. The Magnus Ehrnrooth foundation, Makarna Olins Stipendiefond at the Student Union of Åbo Akademi University and Rector of Åbo Akademi University are gratefully acknowledged for the financial support to OL.

## Notes and references

- 1 M. J. Climent, A. Corma and S. Iborra, *Chem. Rev.*, 2011, **111**, 1072–1133.
- 2 A. Bruggink, R. Schoevaart and T. Kieboom, *Org. Process Res. Dev.*, 2003, **7**, 622–640.
- 3 T. Sehl, H. C. Hailes, J. M. Ward, R. Wardenga, E. von Lieres, H. Offermann, R. Westphal, M. Pohl and D. Rother, *Angew. Chem., Int. Ed.*, 2013, **52**, 6772–6775.
- 4 C. M. R. Volla, I. Atodiresei and M. Rueping, *Chem. Rev.*, 2014, **114**, 2390–2431.
- 5 K. C. Nicolaou, D. J. Edmonds and P. G. Bulger, *Angew. Chem., Int. Ed.*, 2006, **45**, 7134–7186.
- 6 H.-C. Guo and J.-A. Ma, *Angew. Chem., Int. Ed.*, 2006, **45**, 354–366.
- 7 D. Yu. Murzin and R. Leino, *Chem. Eng. Res. Des.*, 2008, **86**, 1002–1010.
- 8 O. Långvik, T. Saloranta, A. Kirilin, A. Liljeblad, P. Mäki-Arvela, L. T. Kanerva, D. Y. Murzin and R. Leino, *ChemCatChem*, 2010, **2**, 1615–1621.
- 9 O. Långvik, P. Mäki-Arvela, A. Aho, T. Saloranta, D. Yu. Murzin and R. Leino, *Catal. Lett.*, 2013, **143**, 142–149.
- 10 I. Busygin, M. Rosenholm, E. Toukoniitty, D. Yu. Murzin and R. Leino, *Catal. Lett.*, 2007, **117**, 91–98.
- 11 T. Tanaka, M. Kawase and S. Tani, *Bioorg. Med. Chem.*, 2004, **12**, 501–505.
- 12 O. B. Wallace, D. W. Smith, M. S. Deshpande, C. Polson and K. M. Felsenstein, *Bioorg. Med. Chem. Lett.*, 2003, **13**, 1203–1206.

- 13 Q. K. Fang, Z. Han, P. Grover, D. Kessler, C. H. Senanayake and S. A. Wald, *Tetrahedron: Asymmetry*, 2000, **11**, 3659–3663.
- 14 W. Adam, M. Lazarus, C. R. Saha-Möller and P. Schreier, *Acc. Chem. Res.*, 1999, **32**, 837–845.
- 15 F. A. Davis and B. C. Chen, *Chem. Rev.*, 1992, **92**, 919–934.
- 16 P. Hoyos, J.-V. Sinisterra, F. Molinari, A. R. Alcántara and P. D. de María, *Acc. Chem. Res.*, 2010, **43**, 288–299.
- 17 C. H. Senanayake, *Aldrichimica Acta*, 1998, **31**, 3–16.
- 18 A. K. Ghosh, S. Fidanze and C. H. Senanayake, *Synthesis*, 1998, 937–961.
- 19 Y. Hong, Y. Gao, X. Nie and C. M. Zepp, *Tetrahedron Lett.*, 1994, **35**, 6631–6634.
- 20 J. Y.-T. Soh and C.-H. Tan, *J. Am. Chem. Soc.*, 2009, **131**, 6904–6905.
- 21 S. Liu and C. Wolf, *Org. Lett.*, 2008, **10**, 1831–1834.
- 22 X. L. Liu, Z. J. Wu, X. L. Du, X. M. Zhang and W. C. Yuan, *J. Org. Chem.*, 2011, **76**, 4008–4017.
- 23 M. Delamare, S. Belot, J. C. Caille, F. Martinet, H. B. Kaagn and V. Hentyon, *Tetrahedron Lett.*, 2009, **50**, 1702–1704.
- 24 Y. Kobayashi, F. Morisawa and K. Saigo, *J. Org. Chem.*, 2005, **71**, 606–615.
- 25 W. Adam, M. T. Díaz, R. T. Fell and C. R. Saha-Möller, *Tetrahedron: Asymmetry*, 1996, **7**, 2207–2210.
- 26 O. Pàmies and J.-E. Bäckvall, *Chem. Rev.*, 2003, **103**, 3247–3262.
- 27 B. Martín-Matute and J.-E. Bäckvall, *Curr. Opin. Chem. Biol.*, 2007, **11**, 226–232.
- 28 J. H. Lee, K. Han, M.-J. Kim and J. Park, *Eur. J. Org. Chem.*, 2010, 999–1015.
- 29 K. Szőri, G. Szöllösi and M. Bartók, *Adv. Synth. Catal.*, 2006, **348**, 515–522.
- 30 B. Stewart, J. Nyhlen, B. Martín-Matute, J.-E. Bäckvall and T. Privalov, *Dalton Trans.*, 2013, **42**, 927–934.
- 31 M. Päiviö, D. Mavrynsky, R. Leino and L. T. Kanerva, *Eur. J. Org. Chem.*, 2011, 1452–1457.
- 32 O. Verho, E. V. Johnston, E. Karlsson and J.-E. Bäckvall, *Chem. – Eur. J.*, 2011, **17**, 11216–11222.
- 33 M. C. Warner, O. Verho and J.-E. Bäckvall, *J. Am. Chem. Soc.*, 2011, **133**, 2820–2823.
- 34 D. Mavrynsky, L. T. Kanerva, R. Sillanpää and R. Leino, *Pure Appl. Chem.*, 2011, **83**, 479–487.
- 35 A. N. Parvulescu, J. Janssens, J. Vanderleyden and D. De Vos, *Top. Catal.*, 2010, **53**, 931–941.
- 36 A. N. Parvulescu, P. A. Jacobs and D. E. De Vos, *Adv. Synth. Catal.*, 2008, **350**, 113–121.
- 37 N. Kim, S.-B. Ko, M. S. Kwon, M.-J. Kim and J. Park, *Org. Lett.*, 2005, **7**, 4523–4526.
- 38 J.-S. Im, S.-H. Ahn and Y.-H. Park, *Chem. Eng. J.*, 2013, **234**, 49–56.
- 39 Y. K. Choi, M. J. Kim, Y. Ahn and M.-J. Kim, *Org. Lett.*, 2001, **3**, 4099–4101.
- 40 N. Ravasio, F. Zaccheria, A. Fusi and R. Psaro, *Phys. Rev. A: At., Mol., Opt. Phys.*, 2006, **315**, 114–119.
- 41 R. Millet, A. M. Träff, M. L. Petrus and J.-E. Bäckvall, *J. Am. Chem. Soc.*, 2010, **132**, 15182–15184.
- 42 S. Sahin, J. Wärnå, P. Mäki-Arvela, T. Salmi and D. Yu. Murzin, *J. Chem. Technol. Biotechnol.*, 2010, **85**, 192–198.
- 43 A. Kirilin, P. Mäki-Arvela, M. Rupp, E. Toukoniitty, N. Kumar, K. Kordas, L. M. Kustov, T. Salmi and D. Yu. Murzin, *Res. Chem. Intermed.*, 2010, **36**, 193–210.
- 44 A. Kirilin, P. Mäki-Arvela, K. Kordas, A.-R. Leino, A. Shchukarev, D. Boström, J.-P. Mikkola, L. M. Kustov, T. O. Salmi and D. Yu. Murzin, *Kinet. Catal.*, 2011, **52**, 72–76.
- 45 A. Kirilin, P. Mäki-Arvela, K. Kordas, A.-R. Leino, A. Shchukarev, D. Boström, J.-P. Mikkola, L. M. Kustov, T. O. Salmi and D. Yu. Murzin, *Kinet. Catal.*, 2011, **52**, 77–81.
- 46 S. Sahin, P. Mäki-Arvela, M. Kangas, K. Eränen, J. Wärnå, T. Salmi and D. Yu. Murzin, *Kinet. Catal.*, 2012, **53**, 673–683.
- 47 P. Lozano, T. de Diego, D. Carrie, M. Vaultier and J. L. Iborra, *Chem. Commun.*, 2002, 692–693.
- 48 H. R. Hobbs, B. Kondor, P. Stephenson, R. A. Sheldon, N. R. Thomas and M. Poliakoff, *Green Chem.*, 2006, **8**, 816–821.
- 49 M. Hartmann and D. Jung, *J. Mater. Chem.*, 2010, **20**, 844–857.
- 50 R. L. Hartman, J. P. Mc Mullen and K. F. Jensen, *Angew. Chem., Int. Ed.*, 2011, **50**, 2–20.
- 51 N. G. Anderson, *Org. Process Res. Dev.*, 2012, **16**, 852–869.
- 52 S. Strompen, M. Weiß, H. Gröger, L. Hilterhaus and A. Liese, *Adv. Synth. Catal.*, 2013, **355**, 2391–2399.
- 53 R. Porcar, V. Sans, N. Ríos-Lombardía, V. Gotor-Fernández, V. Gotor, M. I. Burguete, E. García-Verdugo and S. V. Luis, *ACS Catal.*, 2012, **2**, 1976–1983.
- 54 S. Mascia, P. L. Heider, H. Zhang, R. Lakerveld, B. Benyahia, P. I. Barton, R. D. Braatz, C. L. Cooney, J. M. B. Evans, T. F. Jamison, K. F. Jensen, A. S. Myerson and B. L. Trout, *Angew. Chem., Int. Ed.*, 2013, **52**, 12359–12363.
- 55 M. P. Cava, R. L. Litle and D. R. Napier, *J. Am. Chem. Soc.*, 1958, **80**, 2257–2263.
- 56 O. Petrovskaia, B. M. Taylor, D. B. Hauze, P. J. Carroll and M. M. Joullie, *J. Org. Chem.*, 2001, **66**, 7666–7675.
- 57 S. K. Gupta and S. A. Marathe, *J. Pharm. Sci.*, 1976, **65**, 134–135.
- 58 P. K. Banerjee, D. Mukhopadhyay and D. N. Chaudhury, *J. Indian Chem. Soc.*, 1965, **42**, 115–120.
- 59 Y. Chiang, A. J. Kresge, O. Sadovski, X. Zeng and Y. Zhu, *Can. J. Chem.*, 2005, **83**, 1202–1206.
- 60 L. T. Kanerva and O. Sundholm, *J. Chem. Soc., Perkin Trans. 1*, 1993, 2407–2410.
- 61 K. Yamaguchi, T. Koike, J. W. Kim, Y. Ogasawara and N. Mizuno, *Chem. – Eur. J.*, 2008, **14**, 11480–11487.
- 62 L. M. Neal, S. D. Jones, M. L. Everett, G. B. Hoflund and H. E. Hagelin-Weaver, *J. Mol. Catal. A: Chem.*, 2010, **325**, 25–35.
- 63 R. Ahlrichs, M. Bär, M. Häser, H. Horn and C. Kölmel, *Chem. Phys. Lett.*, 1989, **162**, 165–169.

- 64 M. Von Arnim and R. Ahlrichs, *J. Comput. Chem.*, 1998, **19**, 1746–1757.
- 65 O. Treutler and R. Ahlrichs, *J. Chem. Phys.*, 1995, **102**, 346–354.
- 66 A. D. Becke, *Phys. Rev. A: At., Mol., Opt. Phys.*, 1988, **38**, 3098–3100.
- 67 C. Lee, W. Yang and R. Parr, *Phys. Rev. B: Condens. Matter Mater. Phys.*, 1988, **37**, 785–789.
- 68 A. D. Becke, *J. Chem. Phys.*, 1993, **98**, 5648–5652.
- 69 K. Eichkorn, O. Treutler, H. Öhm, M. Häser and R. Ahlrichs, *Chem. Phys. Lett.*, 1995, **242**, 652–660.
- 70 K. Eichkorn, F. Weigend, O. Treutler and R. Ahlrichs, *Theor. Chem. Acc.*, 1997, **97**, 119–124.
- 71 M. Sierka, A. Hogeckamp and R. Ahlrichs, *J. Chem. Phys.*, 2003, **118**, 9136–9148.
- 72 A. Schäfer, C. Huber and R. Ahlrichs, *J. Chem. Phys.*, 1994, **100**, 5829–5835.
- 73 M. W. Schmidt, K. K. Baldridge, J. A. Boatz, S. T. Elbert, M. S. Gordon, J. H. Jensen, S. Koseki, N. Matsunaga, K. A. Nguyen, S. J. Su, T. L. Windus, M. Dupuis and J. A. Montgomery, *J. Comput. Chem.*, 1993, **14**, 1347–1363.
- 74 W. J. Hehre, L. Radom, P. von R. Schleyer and J. A. Pople, *Ab Initio Molecular Orbital Theory*, John Wiley&Sons, New York, 1986.
- 75 W. J. Hehre, R. Ditchfield and J. A. Pople, *J. Chem. Phys.*, 1972, **56**, 2257–2261.
- 76 P. C. Hariharan and J. A. Pople, *Theor. Chim. Acta*, 1973, **28**, 213–222.
- 77 M. M. Francl, W. J. Pietro, W. J. Hehre, J. S. Binkley, D. J. DeFrees, J. A. Pople and M. S. Gordon, *J. Chem. Phys.*, 1982, **77**, 3654–3665.
- 78 D. E. Bicknell and R. S. Ramotowski, *J. Forensic Sci.*, 2008, **53**, 1108–1116.
- 79 S. Wiesner, E. Springer, Y. Sasson and J. Almog, *J. Forensic Sci.*, 2001, **46**, 1082–1084.
- 80 *Compendium of Chemical Terminology - Gold Book Version 2.3.2; [Online]*, International Union of Pure and Applied Chemistry (IUPAC), Posted, 2012, pp. 97–98, <http://goldbook.iupac.org/> (accessed Dec. 2, 2013).
- 81 N. Tyutyulkov, M. Tasseva and E. Georgiev, *J. Prakt. Chem.*, 1987, **329**, 780–786.
- 82 G. A. Russel, C. L. Myers, P. Bruni, F. A. Neugebauer and R. Blankespoor, *J. Am. Chem. Soc.*, 1970, **92**, 2762–2769.
- 83 E. T. Strom, *J. Org. Chem.*, 1995, **60**, 5686–5689.
- 84 E. T. Strom, E. G. Janzen and J. L. Gerlock, *Mol. Phys.*, 1970, **19**, 577–580.
- 85 L. F. Fieser, *J. Am. Chem. Soc.*, 1948, **70**, 3165–3174.
- 86 K. L. Platt and F. Oesch, *J. Org. Chem.*, 1983, **48**, 265–268.
- 87 P. Ciuffreda, S. Casati and E. Santaniello, *Tetrahedron*, 2000, **56**, 317–321.
- 88 C. Ran, Q. Dai, Q. Ruan, T. M. Penning, I. A. Blair and R. G. Harvey, *J. Org. Chem.*, 2007, **73**, 992–1003.
- 89 D. Mavrynsky, D. Yu. Murzin and R. Leino, *ChemCatChem*, 2013, **5**, 2436–2445.
- 90 B. Martín-Matute, M. Edin, K. Bogár, F. B. Kaynak and J.-E. Bäckvall, *J. Am. Chem. Soc.*, 2005, **127**, 8817–8825.
- 91 M. C. Warner and J.-E. Bäckvall, *Acc. Chem. Res.*, 2013, **46**, 2545–2555.
- 92 P. Ödman, L. A. Wessjohan and U. T. Bornscheuer, *J. Org. Chem.*, 2005, **70**, 9551–9555.
- 93 S. Wuyts, K. De Temmerman, D. E. De Vos and P. A. Jacobs, *Chem. – Eur. J.*, 2005, **11**, 386–397.
- 94 S. Wuyts, J. Wahlen, P. A. Jacobs and D. E. De Vos, *Green Chem.*, 2007, **9**, 1104–1108.
- 95 K. Engström, M. Shakeri and J.-E. Bäckvall, *Eur. J. Org. Chem.*, 2011, 1827–1830.
- 96 F. Zaccheria, N. Ravasio, R. Psaro and A. Fusi, *Chem. – Eur. J.*, 2006, **12**, 6426–6431.
- 97 K. Yamaguchi, T. Koike, M. Kotani, M. Matsushita, S. Shinachi and N. Mizuno, *Chem. – Eur. J.*, 2005, **11**, 6574–6582.
- 98 H. M. Jung, J. H. Koh, M.-J. Kim and J. Park, *Org. Lett.*, 2000, **2**, 2487–2490.
- 99 M.-J. Kim, W.-H. Kim, K. Han, Y. K. Choi and J. Park, *Org. Lett.*, 2007, **9**, 1157–1159.
- 100 H. Haario, *ModEst 6.0, User Guide*, Helsinki, 2010.
- 101 D. Yu. Murzin, N. V. Kul'kova and M. I. Temkin, *Proceeding of the USSR conference on catalyst deactivation, Book of Abstracts*, Ufa, 1989, vol. 2, pp. 85–86.